J Am Soc Nephrol 9: 1213–1224, 1998

In Progressive Nephropathies, Overload of Tubular Cells with Filtered Proteins Translates Glomerular Permeability Dysfunction into Cellular Signals of Interstitial Inflammation

MAURO ABBATE,* CARLA ZOJA,* DANIELA CORNA,* MATTEO CAPITANIO,* TULLIO BERTANI,*† and GIUSEPPE REMUZZI*†

**Mario Negri Institute for Pharmacological Research, Bergamo, Italy; and †Division of Nephrology and Dialysis, Azienda Ospedaliera, Ospedali Riuniti di Bergamo, Bergamo, Italy.*

Abstract. Progression to end-stage renal failure is the final common pathway of many forms of glomerular disease, independent of the type of initial insult. Progressive glomerulopathies have in common persistently high levels of urinary protein excretion and tubulointerstitial lesions at biopsy. Among the cellular mechanisms that may determine progression regardless of etiology, the traffic of excess proteins filtered from glomerulus in renal tubule may have functional importance by initiating interstitial inflammation in the early phase of parenchymal injury. This study analyzes the time course and sites of protein accumulation and interstitial cellular infiltration in two different models of proteinuric nephropathies. In remnant kidneys after 5/6 renal mass ablation, albumin and IgG accumulation by proximal tubular cells was visualized in the early stage, preceding interstitial infiltration of MHC-II-positive cells and macrophages. By double-staining, infiltrates developed at or near tubules containing intracellular IgG or luminal casts. This relationship persisted thereafter despite more irregular distribution of infiltrate. Similar patterns were found in an immune model (passive Heymann nephritis), indicating that the interstitial inflammatory reaction develops at the sites of protein overload, regardless of the type of glomerular injury. Osteopontin was detectable in cells of proximal tubules congested with protein in both models at sites of interstitial infiltration, and by virtue of its chemoattractive action this is likely mediator of a proximal tubule-dependent inflammatory pathway in response to protein load. Protein overload of tubules is a key candidate process translating glomerular protein leakage into cellular signals of interstitial inflammation. Mechanisms underlying the proinflammatory response of tubular cells to protein challenge in diseased kidney should be explored, as well as ways of limiting protein reabsorption/deposition to prevent consequent inflammation and progressive disease.

Chronic diseases of the kidney have an intrinsic tendency to progress to parenchymal scarring and loss of renal function requiring chronic dialysis or transplantation, with an ever-increasing impact on clinical practice and healthcare policy. The most prevalent underlying conditions are glomerulopathies, characterized by both a highly enhanced glomerular permeability to proteins, in turn leading to increased urinary protein excretion, and concomitant tubulointerstitial inflammation and scarring (1). The functional importance of tubulointerstitial events in progressive renal failure is supported by evidence that the severity of tubulointerstitial damage and in particular the macrophage infiltration strongly correlate with the risk of renal progression, even better than the glomerular lesions (1,2). Previous studies on the progressive nature of renal disease have focused on individual inflammatory mediators of tubulointerstitial damage, but "common pathway" cellular mechanisms that may trigger inflammation regardless of initiating nephropathy have not been fully clarified. Among candidate mechanisms, it has been suggested that proteins filtered through the glomerular capillary may have intrinsic renal toxicity, which, together with hypertension and other independent risk factors, would promote progressive renal damage. The scientific basis for this thinking relies on concordant evidence from both animal and human studies (1) that: (*1*) more severe proteinuria is associated with more severe lesions and faster progression; (*2*) low-protein diets or drugs protect the kidney while both ameliorating glomerular permselectivity and preventing the increase in urinary protein excretion; and (*3*) the high protein load on kidney experimentally causes structural parenchymal injury with interstitial accumulation of macrophages and MHC-II-positive cells (1,3). The role of protein toxicity in human nephropathies has been confirmed by recent data relating to the superior protection offered against worsening proteinuria and declining renal function by angiotensin-converting enzyme inhibitors, which may act by limiting the increasingly high glomerular permeability and the consequent filtered protein traffic in the kidney (4).

Recent studies seeking to clarify the mechanisms of renal protein toxicity have generated the hypothesis that the high

Received October 20, 1997. Accepted January 14, 1998.
Dr. Barry Brenner served as Guest Editor and supervised the review and final disposition of this manuscript.
Correspondence to Dr. Mauro Abbate, Mario Negri Institute for Pharmacological Research, Via Gavazzeni 11, 24125 Bergamo, Italy.
1046-6673/0907-1213$03.00/0
Journal of the American Society of Nephrology

load of proximal tubular epithelial cells by filtered proteins may serve as an early trigger of interstitial inflammation. Evidence is based mainly on *in vitro* experiments documenting that the load of proximal tubular cells with albumin or IgG proteins normally abundant in plasma upregulates inflammatory (monocyte chemoattractant protein-1 [MCP-1], RANTES) and vasoactive genes (endothelins) (1,5–7). In the presence of immune glomerulonephritis and/or sustained proteinuria, hormones, growth factors, and proinflammatory proteins (transferrin, insulin-like growth factor-I, complement components) are filtered in tubules, where they can additionally exert proinflammatory or fibrogenic actions (8,9). However, no studies have answered the key questions of whether filtered albumin and other plasma proteins actually cause overload of tubules in areas of subsequent interstitial cellular infiltration, or whether tubular cells at those sites may activate proinflammatory pathways relevant to this response. The aims of the present study were to compare by immunohistochemical techniques the patterns of filtered protein load and interstitial infiltration during the course of experimental proteinuric nephropathies, in order to explore the putative role of altered intrarenal protein traffic in the induction of tubulointerstitial injury.

Materials and Methods

Animals and Disease Models

Male Sprague Dawley CD-COBS rats (240 to 260 g at the beginning of the experiments; Charles River, Calco, Italy) were used. Animal care and treatment were conducted in accordance with institutional guidelines outlined in national and international laws and policies (EEC Council Directive 86/609, OJL 358, December 1987; National Institutes of Health Guide for the Care and Use of Laboratory Animals, National Institutes of Health Publication no. 85-23, 1985). All animals were housed in a room in which the temperature was kept constant on a 12-h light/dark cycle and fed a standard diet. Renal mass ablation was performed by surgical removal of the right kidney and ligation of two or three branches of the left renal artery (10). Three groups of rats ($n = 4$ each group) were sacrificed at 7, 14, and 30 d. Three groups of age-matched rats were used as controls after sham operation, consisting of a laparotomy and manipulation of renal pedicles only. Passive Heymann nephritis (PHN) was induced by a single intravenous injection of 0.5 ml/100 g body wt of rabbit anti-Fx1A antibody, prepared according to Edgington *et al.* (11). The PHN rats were sacrificed at day 7 or month 1, 3, or 10 after disease induction ($n = 4$ each group); age-matched groups of normal rats ($n = 4$ each group) were used as controls for each time point.

Twenty-four hour urine samples were collected in metabolic cages both before the time of disease induction and at each subsequent time point for determination of urinary protein. Proteinuria was determined by the modified Coomassie blue G dye-binding assay for proteins, with bovine serum albumin as standard (12). Results are expressed as mean ± SEM.

At sacrifice, the animals were anesthetized with sodium pentobarbital solution intraperitoneally (0.1 ml/100 g body wt of a 65 mg/ml solution), and the kidneys were fixed by perfusion via abdominal aorta (13). Kidneys were first perfused with Hanks' balanced salt solution for 5 min and then fixed with periodate-lysine paraformaldehyde fixative (14) for 10 min, followed by overnight fixation in the same fixative at 4°C. The fragments from remnant kidneys were taken from the center of noninfarcted areas. Fixed tissue specimens were extensively washed with phosphate-buffered saline (PBS) (0.9% NaCl in 10 mM sodium phosphate buffer, pH 7.4).

Immunohistochemistry

Tissue specimens were immersed in 30% sucrose/PBS for at least 1 h at room temperature, embedded in OCT medium, and frozen in liquid nitrogen. Tissue sections (5 μm thick) were cut using a Mikrom 500 O cryostat (Walldorf, Germany) and either stained immediately or stored at −20°C until further processing. Nonspecific binding of antibodies was blocked with PBS/1% bovine serum albumin (BSA) for 15 min (room temperature) or, for the detection of albumin, PBS/1% gelatin. Albumin was detected with rabbit anti-rat albumin (purified IgG, diluted to 25 μg/ml in PBS; Cappel Laboratories, Durham, NC) (overnight, 4°C), followed by three 5-min washes with PBS (room temperature) and by incubation with tetramethylrhodamine isothiocyanate-conjugated goat anti-rabbit IgG (affinity-purified, 25 μg/ml in PBS; Jackson ImmunoResearch Laboratories, West Grove, PA) for 1 h at room temperature. Rat IgG and rat C3 were stained by direct immunofluorescence with FITC-conjugated goat anti-rat IgG (affinity-purified, 30 μg/ml in PBS; Jackson ImmunoResearch Laboratories) or anti-rat C3 (20 μg/ml; Cappel) for 1 h at room temperature. After final washing with PBS, slides were mounted using 100 mM Tris-HCl:glycerol 50:50, 2% *N*-propyl gallate, pH 8.0. Sections were examined with a Leica DM-R microscope (Wetzlar, Germany) equipped with epifluorescence and appropriate filters. Control experiments for albumin studies, using tetramethylrhodamine isothiocyanate-anti-rabbit IgG alone, resulted in positive staining of tissue sections of 7-d to 1-mo PHN kidneys, due to binding of the secondary antibody to the rabbit anti-Fx1A IgG administered *in vivo*. However, the reactivity was confined to the glomeruli and to the basal aspect of some proximal tubules, and as such it did not affect the evaluation of the patterns produced in tubules by anti-albumin antibody as described below. In any other control experiment in this study, no staining was detectable after incubation with secondary antibodies alone. In additional experiments to control specificity, preabsorption of primary anti-albumin and anti-IgG antibodies with excess purified rat albumin or IgG (Sigma Chemical Co., St. Louis, MO) resulted in complete prevention of staining.

Mouse monoclonal antibodies against a cytoplasmic antigen present in rat monocytes and macrophages (ED-1) (Serotec, Oxford, United Kingdom) (15) or against rat MHC-class II antigen monomorphic determinant on macrophages and dendritic cells, including renal interstitial dendritic cells (OX6) (Sera-Lab, Crawley Down, Sussex, United Kingdom) (16), were used for the localization of infiltrating cells. Tissue sections were blocked with PBS/1% BSA, incubated overnight at 4°C with primary antibody (ED-1, 10 μg/ml; OX6, 10 μg/ml), washed with PBS, and then incubated with Cy3-conjugated donkey anti-mouse IgG antibodies (affinity-purified, absorbed with rat IgG, 5 μg/ml in PBS; Jackson ImmunoResearch) for 1 h at room temperature. For detection of rat osteopontin, a murine monoclonal antibody (MPIIIB10, Developmental Studies Hybridoma Bank, University of Iowa, Iowa City) (17) was used (1 μg/ml) under the same conditions of incubation. Double immunofluorescence labeling was performed by the following sequences: mouse monoclonal (ED-1, OX-6, or MPIIIB10), Cy3-anti-mouse IgG, and either FITC-anti-rat IgG or FITC anti-rat C3. Absence of cross-reactions between antibodies was further confirmed by comparing individual patterns on adjacent sections, and after inversion of the incubation sequences.

Semiquantitative analysis of proximal tubular IgG staining and of MHC-II-positive cells was performed by examining randomly selected microscopic fields (×400) of cortical tubulointerstitial areas in

double-stained sections. In each field (mean number of fields for each animal, 23; range, 14 to 33), the proximal tubules were counted and the staining intensity for each tubule was graded as follows: 0, absent; 1, low; 2, moderate; and 3, high. The number of cells displaying MHC-II staining was counted in the same fields. Results are expressed as percentage of proximal tubules with a score of 1, 2, or 3, and as average number of MHC-II-positive cells per field. The number of tubular casts was counted in microscopic fields (×100) covering approximately 70% of the cortical area in each section.

Immunoelectron Microscopy

Fragments of periodate-lysine paraformaldehyde-fixed renal cortex were infiltrated with 2.3 M sucrose for at least 1 h and sectioned at approximately −100°C, using a Reichert FCS ultracryomicrotome (18). Well preserved proximal tubules were selected after examination of semithin frozen sections from two normal kidneys and two 14-d remnant kidneys, and at least 10 proximal tubular profiles were analyzed from each kidney. Ultrathin sections were stored at 4°C on 1% gelatin in PBS until use and were incubated overnight (4°C) with either rabbit anti-rat albumin antibodies (25 μg/ml), followed by 1 h (room temperature) in protein A conjugated to colloidal gold as described previously (13), or with goat anti-rat IgG coupled to 10-nm gold particles (Amersham, Buckinghamshire, England, United Kingdom). After washes in PBS, sections were fixed for 10 min in 1% glutaraldehyde, washed again in distilled water, and stained for 5 min with 2% aqueous uranyl acetate. They were then destained and embedded in methylcellulose before examining with a Zeiss EM109 electron microscope.

Results

Patterns of Albumin and IgG Traffic in Kidney

Normal Rat Kidney. The examination at low magnification of cryostat sections of kidney cortex from normal rats revealed staining in the proximal tubules with anti-albumin antibody. The main pattern was vesicular and granular at the base of brush borders, with strong intensity of staining in some profiles and very weak staining in others (Figure 1A). Tubular cells at higher magnification showed intracellular granular reactivity of lysosome-like structures in the cytoplasm. A small amount of albumin was observed in glomeruli, with granular patterns in regions corresponding to podocytes and mesangial areas, as well as in tubular basement membranes and the amorphous matrix. IgG staining was only detectable in sparse cells of proximal tubules, showing a weak subapical or irregular granular pattern, and in glomeruli with punctate or granular distribution in mesangial areas (Figure 1B).

Remnant Kidney. Rats with remnant kidneys developed progressively higher levels of urinary protein excretion after surgery (in mg/d): 7 d, 53.6 ± 9.7; 14 d, 142.7 ± 26.6; 30 d, 253.3 ± 66.1; sham-operated rats, 7 d, 24.6 ± 2.1). In parallel, profound changes were found in kidneys in the staining patterns for both albumin and IgG. In 7-d remnant kidneys, albumin reactivity was localized to proximal tubules, similar to the tubular distribution of albumin in normal kidney; however, tubular profiles displayed an irregular intracellular pattern (Figure 1C) rather than a distinct subapical ring of fluorescence at the base of the brush border. The glomeruli displayed segmental albumin reactivity in granular or less well organized deposits at the periphery of tufts and in mesangial areas.

In contrast to the control kidneys, the inspection of cryostat sections of 7-d remnant kidneys also revealed focal IgG staining both in tubules and glomeruli at low magnification (Figure 1D). IgG protein was localized to proximal tubules, where it concentrated at the base of brush borders and within cytoplasmic granules in the epithelial cells. The IgG staining showed differences in intensity among 7-d remnant kidneys, with very weak reactivity in the kidney taken from a rat that had not developed proteinuria at this time. In glomeruli, the IgG protein deposition was focal and segmental in epithelial cells at the periphery of tufts and in mesangial areas (Figure 1D). In analogy with the albumin pattern, part of such glomerular IgG staining was in cytoplasmic vesicles or granules consistent with epithelial protein reabsorption droplets by histology. Staining for both albumin and IgG was also detectable in a few casts in tubular lumina, vascular poles of glomeruli, and walls of arteries and afferent arterioles.

The 14-d remnant kidneys revealed immunofluorescence patterns for albumin and IgG that overall were similar in cellular distribution to those seen in 7-d remnant kidneys, but with differences in the relative intensity of staining and proportion of structures stained (Figure 1, E and F, and Table 1). Thus, greater proportions of proximal tubules at 14 d exhibited bright intracellular albumin and IgG protein staining; in other tubules, this was either weak or heterogeneous within individual profiles. Some glomeruli and the tubular casts were strongly reactive for both proteins.

Heterogeneous distribution of albumin and IgG protein in tubules persisted in sections of 30-d remnant kidneys (Figure 1, G and H, and Table 1). In addition to tubules showing a strong granular staining, the prevalent pattern in proximal tubules was the presence of a small amount of irregular staining. Also, luminal casts were more frequent, and some cells with granular intracellular albumin and IgG were seen in the lumina of atrophic or dilated tubules. Glomeruli exhibited strong staining, either segmental or global in distribution. The amorphous extracellular matrix stained for both albumin and IgG in focal areas. Kidneys taken from sham-operated rats at any time point showed no differences in the albumin and IgG staining compared with normal control animals.

Ultrastructural Localization of Albumin in Proximal Tubular Epithelial Cells

Immunogold labeling of ultrathin frozen sections of normal proximal tubules revealed material reactive with albumin antibodies in subapical vacuoles of proximal tubular cells, preferentially associated with the inner side of the vesicular membrane. Gold particles were also detectable in some lysosomes in proximal tubular cells (Figure 2, a and c).

In remnant kidneys, lysosome-like structures accumulated in the cell cytoplasm of proximal tubular cells (Figure 2b). Immunogold labeling on sections of 14-d remnant kidneys confirmed the presence of filtered albumin concentrated in cytoplasmic protein reabsorption droplets, often near the nucleus (Figure 2d). In contrast to the normal kidney, abundant immunogold labeling for rat IgG was also present in lysosomes of proximal tubular cells in 14-d remnant kidneys (not shown).

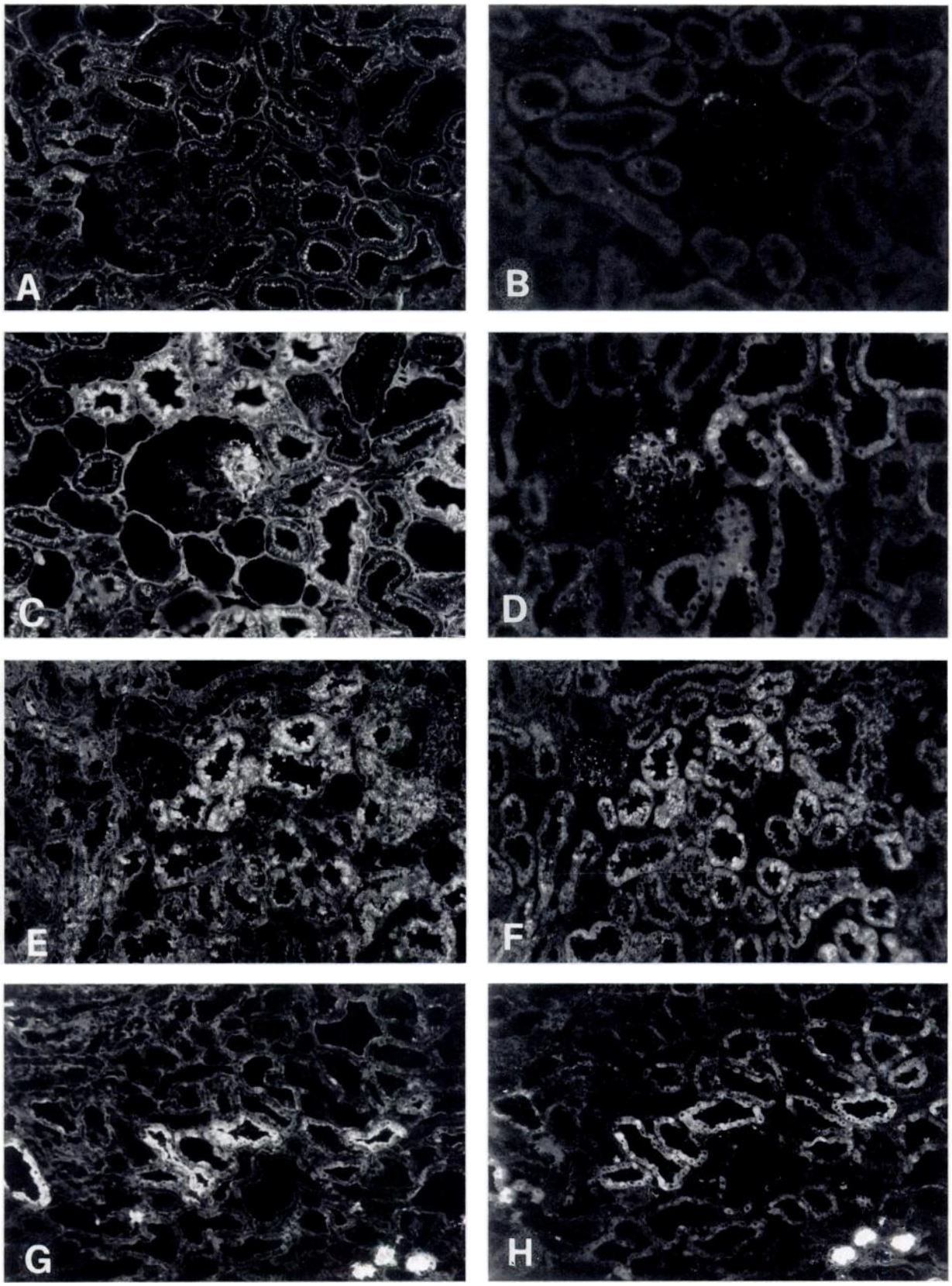

Figure 1. Time course of filtered plasma protein traffic (albumin, left panels; IgG, right panels) in kidney in early stages of disease after 5/6 renal mass ablation. Normal rat kidneys, as well as sham-operated control animals at any time point (as illustrated here at day 7), showed subapical distribution of albumin in proximal tubules (A) and trace or no IgG (B) (Magnification, ×250). In contrast, in 7-d remnant kidneys, proximal tubules exhibited bright and more diffuse albumin (C) and IgG staining (D); glomeruli stained with a focal and segmental pattern (Magnification, ×250). At 14 d, staining was intense and more diffuse in proximal tubular cells; amorphous extracellular matrix also stained

Table 1. Extent and intensity of IgG protein staining in proximal tubules (PT), tubular casts, and MHC-II-positive cells[a]

Group	Day	PT Staining			Casts	MHC-II$^+$ Cells
		1+	2+	3+		
Sham-operated	7	5	0	0	0	4
Remnant kidney	7	24	3	0	0	7
Remnant kidney	14	37	16	8	1	22
Remnant kidney	30	48	22	13	2	32

[a] The proximal tubular staining is expressed as average percentage of profiles (assigned a score of 1+, 2+, or 3+)/total number of proximal tubules (see Materials and Methods). Casts and MHC-II-positive cells are average numbers per field of tubulointerstitial area (examined at magnifications of ×100 and ×400, respectively).

Comparison of the Sites of High Filtered Protein Load in Tubules and Interstitial Cellular Infiltrates in Remnant Kidney

To identify interstitial infiltrates, sections were stained for either ED-1 antigen (rat monocytes/macrophages) or MHC-II antigen expressed at high levels in tubulointerstitial inflammatory infiltrates of proteinuric disease (3). As also described in detail by others, MHC-II-positive cells can be detected with OX6 monoclonal antibody in peritubular interstitium in the rat kidney cortex, and they recently have been characterized as interstitial dendritic cells (16). In contrast, ED-1-positive cells are rare in the cortical interstitium of normal kidney, whereas they are mainly found in small numbers in perivascular areas vessels at the border with the medulla.

Inspection of sections of 7-d remnant kidneys revealed no obvious changes in the distribution of MHC-II-positive cells and no evident infiltrates of ED-1-positive cells. At high magnification, there were only a few small aggregates of MHC-II-positive cells in the cortical interstitium (red fluorescence in Figure 3C, MHC-II, compare with control kidney in b). The interstitial infiltrates became clearly detectable in all sections of 14-d remnant kidneys and then more evident at 30 d (Figure 3, MHC-II in D through E, and ED-1 in F). Infiltrates were dense in some areas, as shown by previous studies (19), and strongly MHC-II-positive. Less dense infiltrates were also found in 30-d remnant kidneys, invariably displaying high levels of MHC class II expression and with irregular or peritubular distribution. In serial sections, it was evident that the interstitial infiltrates consisted of both ED-1 monocytes/macrophages and of cells strongly stained for MHC-II antigen. However, the respective distribution of ED-1 or MHC-II antigens did not overlap completely within the infiltrates (Figure 3, E *versus* F), suggesting that other cells, in addition to monocytes/macrophages, may contribute to the inflammatory infiltrate, possibly including interstitial dendritic cells. MHC-II antigen was detected both in intracellular compartments and on the surface of cells with dendritic-like morphology in semithin frozen sections of the infiltrates (Figure 3G). A dissociation between high MHC-II expression and monocyte infiltration was found in the glomeruli, which were often infiltrated by high numbers of ED-1-positive cells not bearing detectable MHC-II antigen.

To compare the distribution of the tubular sites of filtered protein load and of interstitial infiltrates, sections of remnant kidneys were double-immunostained for IgG (green fluorescence in Figure 3) and MHC-II antigen. Rat IgG was selected as a marker to localize filtered protein because the staining was readily detectable in the regions of accumulation. These experiments revealed that infiltrating cells concentrated early and preferentially in those regions. In 14-d remnant interstitium (Figure 3D), the infiltrating MHC-II-positive cells were predominant in areas in which proximal tubules exhibited intracellular IgG staining, and at some of the tubules with luminal casts. Infiltrates were much less frequent in tubulointerstitial areas, displaying no signs of protein overload in tubular epithelium. In 30-d remnant kidneys, infiltrates of MHC-II-positive cells were also closely associated with tubular sites of protein accumulation, particularly the IgG-positive proximal tubules and the tubules with casts in periglomerular region. The relationship with adjacent proximal tubules containing intracellular IgG protein was still evident at this time despite more diffuse infiltration of MHC-II-positive cells in cortex (Figure 3H). Dense infiltrates were also localized in tubulointerstitial areas showing IgG staining of amorphous extracellular matrix. ED-1 monocytes/macrophages (Figure 3F) were identified in the same tubulointerstitial regions and had similar relationships as the MHC-II-positive cells (Figure 3E), with structures stained for IgG protein. The results of the semiquantitative analysis (Table 1) confirmed that the extent of IgG staining in proximal tubules and the number of casts in tubular lumina progressively increased in parallel with the number of infiltrating MHC-II-positive cells in the same tubulointerstitial areas.

Additional experiments were performed to determine whether complement deposition/accumulation occurs along with IgG in proximal tubules in areas of early tubulointerstitial

for albumin in focal areas (E and F; magnification, ×125). At 30 d, heterogeneous patterns in tubular cells were associated with more frequent casts in tubules (G and H; magnification, ×125). Sections of periodate-lysine paraformaldehyde-perfused kidneys, stained with rabbit anti-rat albumin followed by tetramethylrhodamine isothiocyanate-anti-rabbit IgG, or with FITC-goat anti rat IgG, are shown.

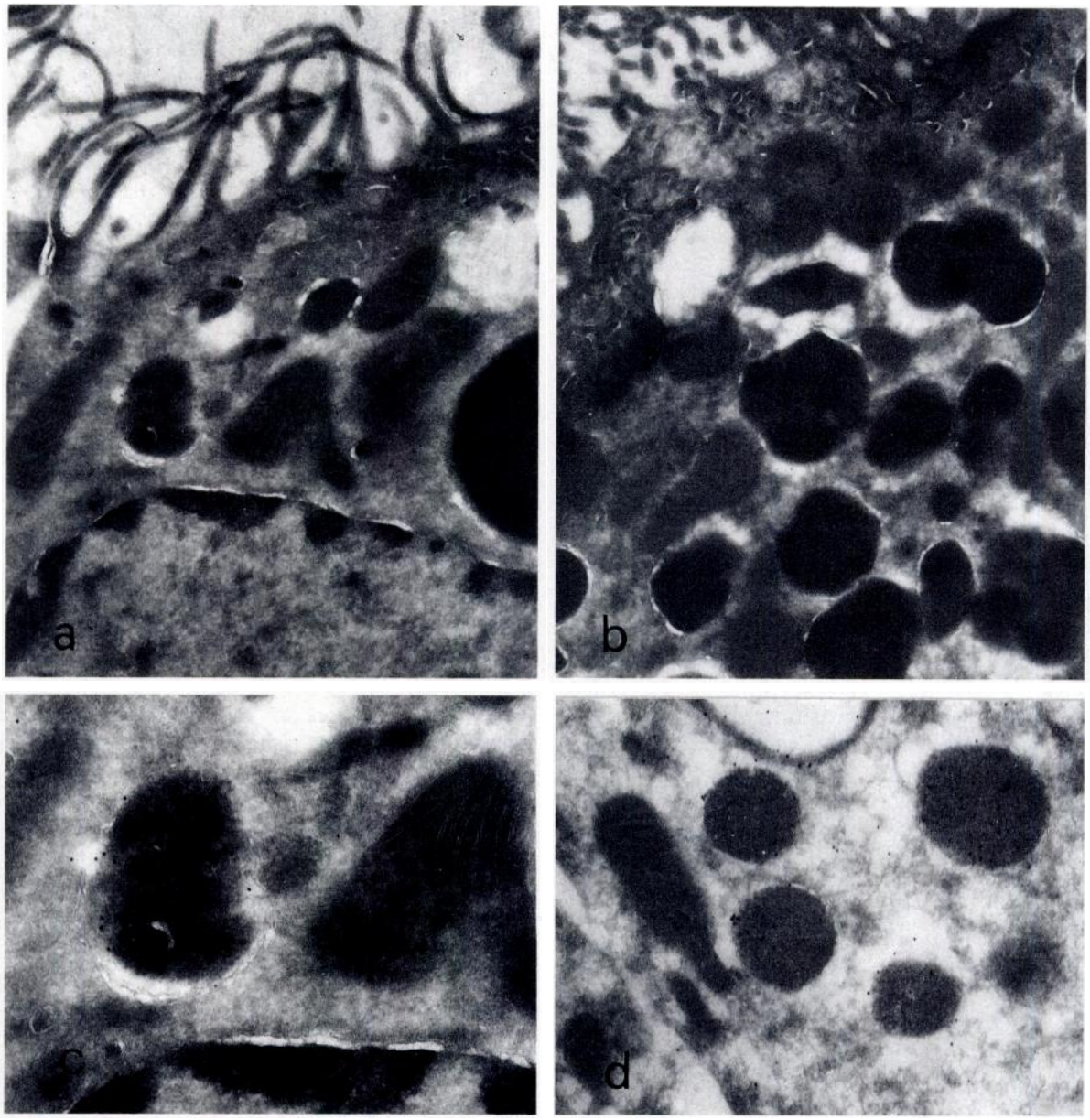

Figure 2. Immunogold labeling of albumin on ultrathin cryosections of proximal tubules. Labeling was present in subapical vacuoles and lysosomes within proximal tubular epithelial cells in normal kidney (a and c) and more evident in 14-d remnant kidney, in which protein reabsorption droplets were abundant in cell cytoplasm (b and d). Magnification: ×7,000 in a and b; ×20,000 in c and d.

infiltration. Both in 14-d and 30-d remnant kidneys, focal C3 reactivity was found in the brush border or within cytoplasmic granules in proximal tubular cells, or both. A linear, circumferential pattern along basement membranes was also found, in contrast to the interrupted staining found focally in the normal kidney. Comparison of the C3 distribution pattern with that of IgG/MHC-II in adjacent sections revealed colocalization of intracellular C3 and IgG to proximal tubular regions in association with MHC-II-positive infiltrates.

Plasma Protein Traffic and Interstitial Inflammation in Kidneys of Rats with Passive Heymann Nephritis

The time course of proteinuria ([in mg/d]: 7 d, 75.8 ± 12.8; 1 mo, 182 ± 47; 3 mo, 336 ± 6; 10 mo, 699 ± 24.4; basal, 22.6 ± 0.9) and renal lesions in rats with passive Heymann nephritis evolved more slowly than in rats with renal mass ablation. Despite major differences in type of initial insult between the two models, the spatial relationships between plasma protein traffic in tubules and interstitial cellular infiltrates were remarkably similar (Figure 4). Analysis of albumin and IgG in cryostat sections of 7-d PHN kidneys revealed bright granular staining in proximal tubules. The abnormal pattern persisted in 1- to 3-mo PHN kidneys, which, in addition to granular IgG deposits along glomerular capillary walls typical of PHN, also developed more evident albumin and IgG reactivity in protein reabsorption droplets in glomeruli and tubular casts. In 10-mo PHN kidneys, albumin and IgG staining was either strong or irregular in greater proportions of

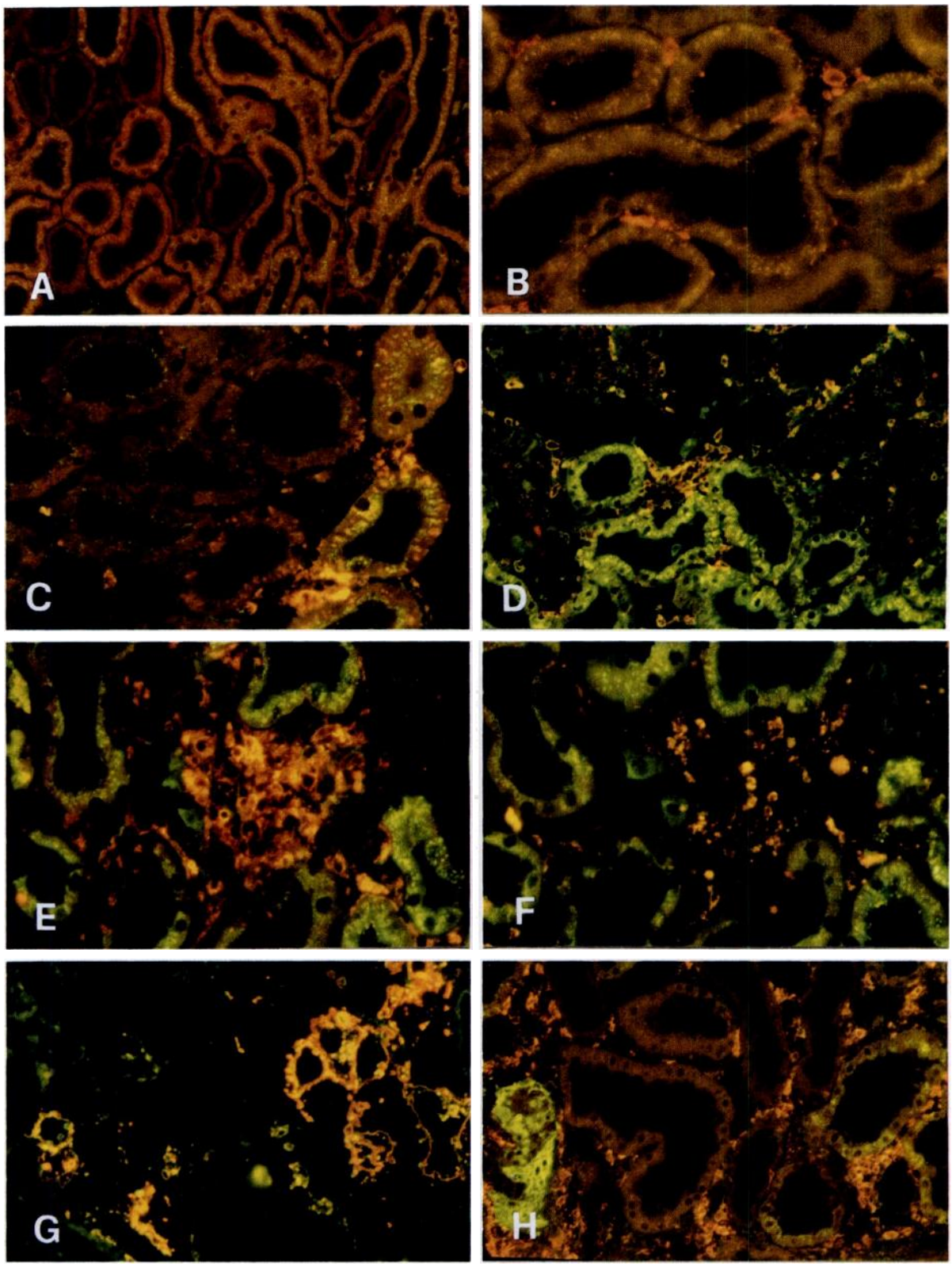

Figure 3. Analysis of interstitial cellular infiltrates and relationship with sites of filtered protein accumulation in remnant kidneys (red and green fluorescence, respectively, on the background of parenchymal structures). In the interstitium of normal kidney, ED-1 macrophages are rare or absent (A; magnification, ×125) and MHC-II-positive cells only sparse (B; magnification, ×250). Seven-day remnant kidneys showed normal patterns, with the exception of occasional small cellular aggregates in the interstitium (C; MHC-II; magnification, ×250). In contrast, interstitial cellular infiltrates were invariably present in 14-d (MHC-II in D, E, and G; ED-1 in F) and in 30-d remnant kidneys (MHC-II in H). Infiltrating cells were localized at or near proximal tubular regions showing intracellular IgG (as seen in B at 14 d) and tubular casts. This relationship persisted at 30 d despite the more irregular distribution of infiltrates (H; magnification, ×125). Infiltrating cells stained brightly for MHC-II antigen, and on serial sections of individual infiltrates (compare MHC-II antigen in E and ED-1 in F; magnification, ×250) the ED-1-positive

proximal tubules; luminal casts in cortical tubules were more frequent, as were foci of amorphous matrix that stained positive for the plasma protein markers.

In double-immunostained sections of 7-d PHN kidney cortex, infiltrates of monocyte/macrophages or MHC-II-positive cells were predominant in areas of proximal tubules displaying intracellular staining for endogenous IgG protein, and much less frequent or absent in the other interstitial areas (Figure 4, A through D). At 1- to 3-mo PHN, interstitial infiltrates had partially subsided, but when present they strictly localized to tubulointerstitial areas showing IgG-positive staining. At 10-mo PHN, chronic inflammatory infiltrates became evident, again exhibiting preferential association of infiltrating cells at sites of IgG-positive proximal tubules and tubular casts (Figure 4, E through H).

Osteopontin in Tubular Epithelium of Proteinuric Rats Is Upregulated at Sites of High Protein Reabsorption and Interstitial Inflammation

Among cytokines relevant to the attraction of mononuclear cells into the renal interstitium, osteopontin has been recently shown to be upregulated in tubular epithelium of proteinuric rats and associated with sites of monocyte/macrophage accumulation (20,21). To determine whether a similar association at those sites also occurs between excess plasma protein reabsorption and osteopontin expression, sections of 14-d remnant kidneys and 10-mo PHN kidneys were double-stained for IgG and osteopontin, and the staining patterns were compared with those of adjacent sections double-stained for IgG and MHC-II antigen.

In tubules of normal rat kidneys, osteopontin staining was found only in the epithelium of occasional distal tubular segments with granular intracellular pattern. In contrast, in PHN and in remnant kidneys, bright intracellular osteopontin staining was present in the proximal tubules with focal distribution. By comparison of serial sections, osteopontin localized to proximal tubular cells showing IgG protein staining, and the sites of colocalization were strictly associated with adjacent interstitial infiltrates (Figure 5). In most of the positive tubules, osteopontin staining was present throughout the tubular cells, and it was usually bright in cells showing bright intracellular IgG staining. In addition, osteopontin was found in cells of distal tubular segments containing casts or showing signs of atrophy and thickened basement membranes; as expected from the above results, these regions were also the sites of MHC-II-positive infiltrates. In both models, some tubular profiles showed IgG and/or osteopontin staining in the absence of infiltrates; however, proximal tubules devoid of IgG and/or osteopontin staining were almost invariably devoid of adjacent or surrounding cellular infiltrates.

Discussion

This study documents that in experimental proteinuric nephropathies, the traffic of filtered plasma proteins leads to excess protein load in proximal tubules at sites of subsequent tubulointerstitial inflammation. In a first set of experiments, we identified the proximal tubule as the initial site of altered plasma protein traffic in tubulointerstitium after 5/6 renal mass ablation. In this model, the primary insult to the kidney is nonimmune in nature, and the altered glomerular permselectivity and proteinuria are associated with compensatory increases in glomerular pressure and flow (10,22,23). That the abnormal albumin and IgG staining in tubules did reflect uptake of filtered proteins as a result of altered glomerular permselectivity was indicated by the presence in remnant glomeruli of segmental protein deposits and reabsorption droplets, absent in normal kidneys and showing impressive analogies with the distribution of glomerular sclerotic lesions that develop thereafter. The hyperfunctional proximal tubules in 7-d remnant kidneys were in all likelihood in a phase of relatively efficient enhanced reabsorption of filtered proteins, such that the signs of high protein load of tubules were associated with a limited degree of proteinuria. Relevant to this point is also the observation that in normal kidneys, albumin staining concentrated in cortical segments of the proximal tubule, in which the reabsorption rates from tubular fluid are theoretically the highest. This was in partial apparent contrast to the uniform high expression of apical albumin-binding molecules (albumin-binding protein and gp330) along the whole length of the proximal tubule (24), but the combined patterns support a high reabsorption potential by the proximal tubule (25) that can be further exploited upon protein load. Lysosomal activity of proximal tubules is also enhanced in nephrosis (26), and we confirmed by immunogold studies the lysosomal localization of filtered proteins to reabsorption droplets in the proximal tubular cells. The subsequent patterns of protein traffic and urinary excretion in 14-d and 30-d remnant kidneys overall defined a transition from initial tubular reabsorption to proximal epithelial cell overload with proteinuria and cast formation. The bright staining for both plasma proteins in luminal casts, often associated with irregular intracellular staining in proximal tubules, clearly reflects impaired reabsorption. In addition, staining of amorphous extracellular matrix, as also reported for exogenous bovine albumin in rats with overload proteinuria (3), would suggest that the abnormal protein traffic, if massive, may determine protein leakage toward the interstitium.

The main findings of this study relate to the temporal and spatial relationships of the events of cellular inflammation with those of altered protein traffic in kidney. The early phase of high protein reabsorption at 7-d after renal ablation preceded the onset of interstitial inflammation. Thus, tubulointerstitial

cells were a major component; in semithin sections (G, counterstained with FITC-wheat germ agglutinin lectin; magnification, ×500), intense MHC-II labeling was also apparent at the surface of cells displaying heterogeneous dendritic-like morphology. For double-staining, sections were incubated with mouse ED-1 or anti-MHC-II, followed by Cy3-donkey anti-mouse IgG, and by FITC goat anti-rat IgG.

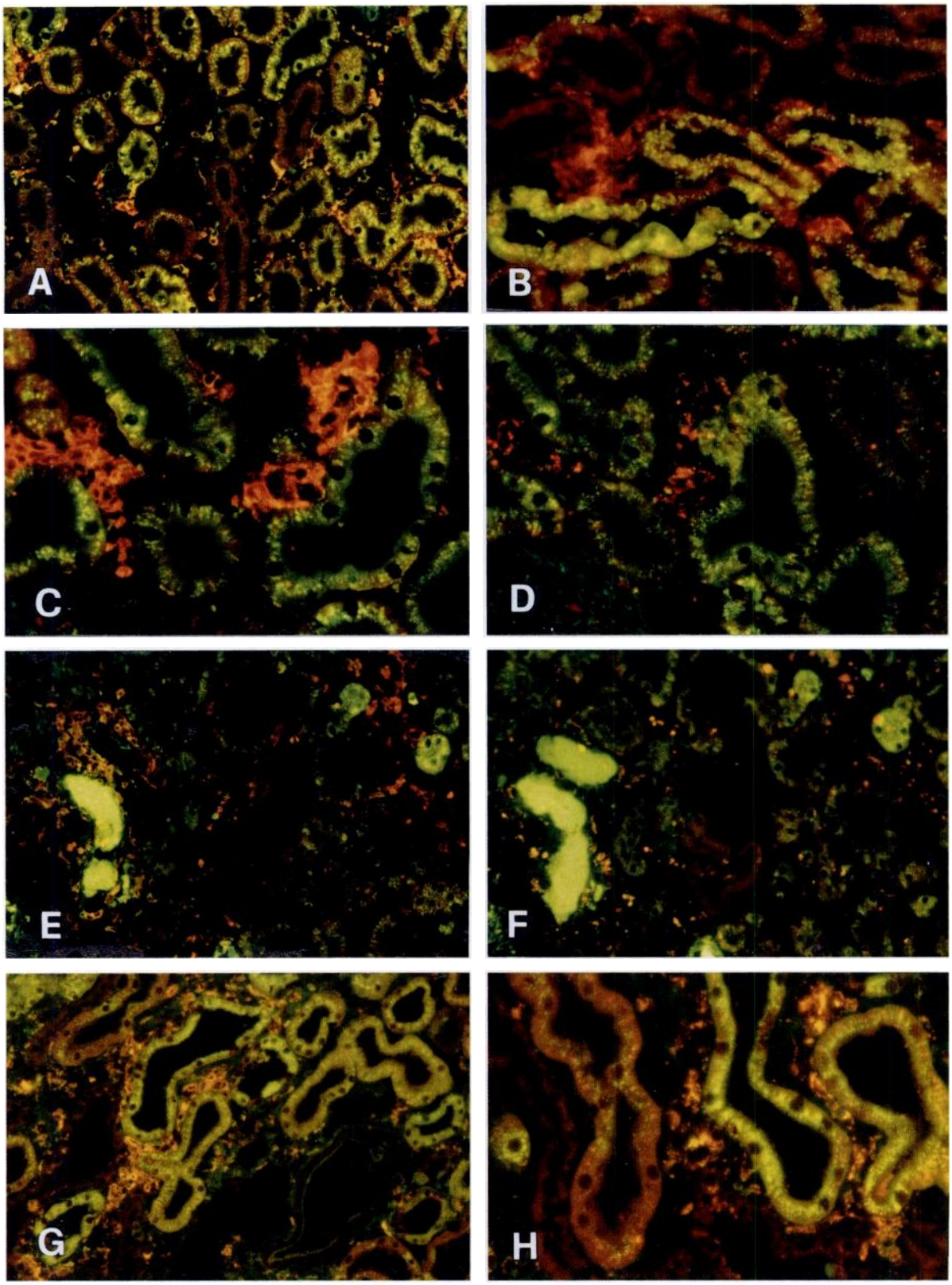

Figure 4. Protein traffic (IgG) and tubulointerstitial infiltration in kidney during early autologous phase (day 7; A through D) or chronic disease (month 10; E through H) of passive Heymann nephritis. The strict spatial relationships of cellular infiltrates (red fluorescence: MHC-II in A, B, C, E, and G; ED-1 in D, F, and H) with sites of plasma protein staining in tubules (green) in both phases are indistinguishable from those seen in remnant kidney (compare with Figure 3), indicating that infiltrating cells accumulate at tubulointerstitial sites of high filtered protein load regardless of the type of initiating glomerular injury. Similarly, ED-1 monocytes/macrophages are major components of MHC-II-positive infiltrate at any time point by comparison on serial sections (compare MHC-II antigen in C, E, and G and ED-1 in D, F, and H). Magnification: ×125 in A, E, F, and G; ×250 in B, C, D, and H.

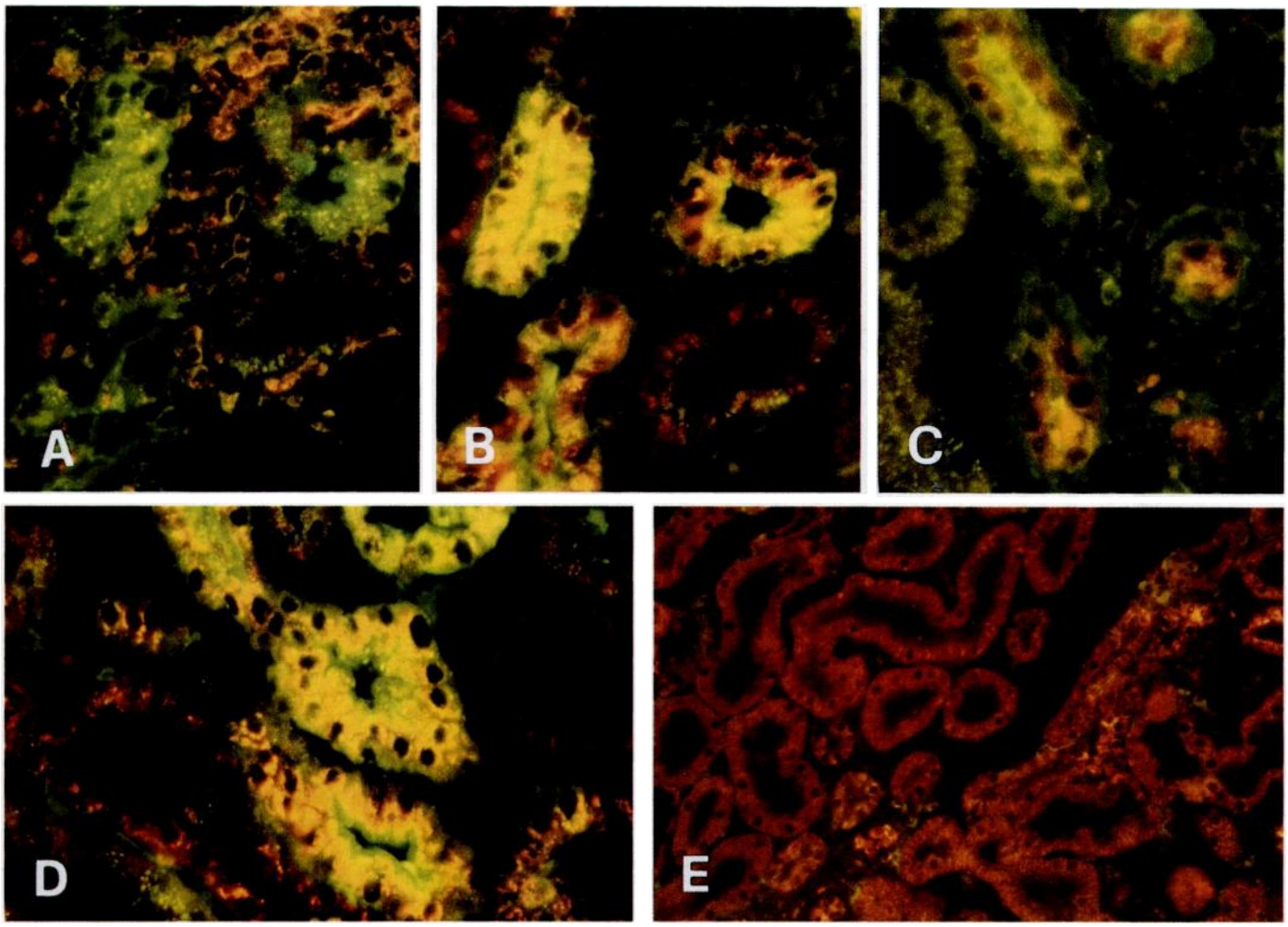

Figure 5. Protein traffic and osteopontin expression in remnant kidney (A through C) and in passive Heymann nephritis (D). By its chemoattractive action, osteopontin may have role in the interstitial inflammatory response to altered protein traffic. (A and B) Fields of the same area (Magnification, ×250) in serial sections of 14-d remnant kidney double-labeled for either IgG and MHC-II antigen (A) or IgG and osteopontin (B). The bright yellow color in B reflects colocalization of osteopontin and IgG (due to overlapping of the respective red and green fluorescence signals) to proximal tubules in an area of tubulointerstitial infiltration. (C) Osteopontin was also detected in tubules containing casts or showing signs of atrophy (Magnification, ×250). (D) Similar colocalization pattern of osteopontin and IgG to proximal tubules in passive Heymann nephritis (10 month) (Magnification, ×250). (E) Control rat kidney (Magnification, ×125).

infiltrates displaying high MHC-II expression and enriched with ED-1 monocytes/macrophages were first detectable in 14-d remnant kidneys and then more evident at 30 d. In double-stained sections, the infiltrating cells concentrated almost exclusively in regions containing IgG-positive proximal tubules and tubules with casts, and conversely they were much less frequent in other tubulointerstitial areas. The cellular infiltrates in 30-d remnant kidneys were more irregular but again closely associated with proximal tubular regions of high filtered protein load. These findings provide for the first time strong morphologic evidence *in vivo* implicating the excess protein reabsorption by proximal tubular cells as an early process possibly instrumental to the development of interstitial inflammation. This is followed by interstitial cellular reaction to luminal protein deposition in distal nephron segments with more irregular distribution of infiltrate. Our data of C3 staining along with IgG in proximal tubular cells also reinforce the role of excess filtered C3 in the induction of tubulointerstitial inflammation, as suggested by previous studies of models of proteinuric nephropathies (3,27,28).

Renal disease of rat remnant kidney is severe and rapidly progressive after the abrupt and massive nephron loss. Human nephropathies usually evolve more slowly and after prolonged periods of sustained proteinuria. To characterize the relationship of high filtered protein load and interstitial inflammation in an immune model that mimics human disease, we analyzed the kidneys of rats with passive Heymann nephritis, an experimental form of membranous glomerulopathy. Glomerular injury is induced by heterologous antibodies (anti-Fx1A) that upon binding to glomerular podocytes cause local formation of immune deposits and proteinuria. A first peak of tubulointerstitial disease between 7 and 14 d in proteinuric rats is attributed to mechanisms driven by heterologous anti-Fx1A antibodies that react with proximal tubules. We found that proximal

tubules exhibited strong irregular staining for albumin and rat IgG, with focal distribution strikingly similar to that seen in remnant cortex, and that the sites of enhanced protein load were also those of interstitial monocyte/macrophage and MHC-II-positive cell accumulation, further suggesting that tubulointerstitial inflammation develops at sites of enhanced protein reabsorption in proximal tubule even after immune glomerular insults. Any form of glomerulonephritis is actually associated with proteinuria and tubulointerstitial inflammation, and the present results suggest that in acute nephritis, the traffic to proximal tubules of a diversity of filtered circulating proteins, nephritogenic antibodies, complement proteins, and cytokines of glomerular origin is a common mechanism leading to activation of pathways of tubulointerstitial injury in different settings.

Chronic disease with sustained proteinuria and progressive tubulointerstitial inflammation develops over several months in PHN following the immune heterologous phase (29), presumably as a consequence of a secondary (autologous) phase of injury in which host rat antibodies react with the heterologous anti-Fx1A antibodies planted along the glomerular capillary wall. Our findings that the tubulointerstitial inflammatory infiltrates first developed in close association with regions of proximal tubules exhibiting signs of excess protein reabsorption at any time point of disease confirm that protein accumulation in tubules precedes and occurs at sites of chronic tubulointerstitial inflammation even after the initial insult to the glomerulus has ceased. In addition, in contrast to the rapid sequence of events shown in the remnant kidney, it seems that in a condition that mimics a form of human proteinuric nephropathy, the protein load of tubules must become both massive (molecules the size of IgG in this study) and sustained after the acute phase.

The above similar patterns in the two models also provide strong morphologic evidence that the high filtered protein load may activate proximal tubule-dependent pathways of interstitial inflammation. Our data are relevant to the attraction of mononuclear cells into interstitium, one of the initial steps in progressive tubulointerstitial disease. Responsible for cell recruitment at sites of excessive protein reabsorption may be a growing number of proinflammatory molecules, with chemoattractive action of the type of MCP-1, RANTES, and osteopontin shown to be upregulated by protein overload of proximal tubular cells (1,5,7,21). Osteopontin staining by immunohistochemistry strictly correlated with mRNA expression by *in situ* hybridization (17), and both are absent in normal proximal tubule. Recent studies have disclosed anatomic relationships between tubular sites of osteopontin synthesis and interstitial infiltrates shared by different models of proteinuric disease (17,20,21). We found that a link in proximal tubules also exists between protein accumulation and osteopontin expression. Thus, osteopontin was localized to proximal tubular cells showing bright IgG protein staining both in remnant kidneys and in rats with passive Heymann nephritis, and the sites of colocalization revealed strict relationships with adjacent infiltrates. These findings indicate that in proximal tubules, the augmented filtered protein load may upregulate osteopontin, in turn promoting macrophage recruitment into adjacent interstitium. In addition, we detected osteopontin in cells of tubules containing casts and in distal tubular segments. Osteopontin upregulation in distal segments may be part of the cellular response to tubular obstruction (30) by luminal casts, leading to additional mononuclear cell infiltration in the environment of proteinuric nephrons. With the present background in such different models, data of colocalization establish links at the cellular level between a common process of progressive nephropathy, namely the accumulation of protein in tubule, as shown here, and both the expression of a chemoattractant molecule and the relevant interstitial inflammatory reaction. Additional studies are needed to determine whether osteopontin is upregulated in proximal tubules in the context of a more general response to intracellular protein congestion. For example, in other cells, the accumulation of proteins in endoplasmic reticulum activates transcription of NFκB-dependent genes for cytokines and adhesion molecules (31), and among NFκB-dependent genes, MCP-1 and RANTES (5,7) are upregulated by protein stress in proximal tubular cells. Such a mechanism would be very similar to that used in the antiviral response by infected cells when viral proteins accumulate in large amounts in the endoplasmic reticulum (31).

In summary, this study demonstrates in two different models of progressive renal disease that plasma proteins abnormally filtered due to altered glomerular permselectivity accumulate in proximal tubular epithelial cells and in tubular lumina, followed by local interstitial infiltration of MHC-II-positive cells. During this process, macrophages and possibly interstitial dendritic cells are recruited at regions of protein overload, at least in part by osteopontin-dependent mechanisms. These data provide conclusive support to the role of altered protein traffic in the induction of tubulointerstitial inflammation and implicate the persistently high protein load of tubule as the missing link, long suspected but hitherto unrecognized at the cellular level, of the common pathway theory of renal disease progression independent of etiology. Given the role of chronic tubulointerstitial injury in subsequent scarring and renal function impairment, the intracellular congestion and luminal deposition of proteins in tubules, as well as downstream cellular signaling and cytokine pathways, should be considered as possible target mechanisms to inhibit, in future approaches, progressive disease even after glomerular permselectivity is irreversibly disrupted.

References

1. Remuzzi G, Ruggenenti P, Benigni A: Understanding the nature of renal disease progression. *Kidney Int* 51: 2–15, 1997
2. Jackle I, Gunther H, von Gise H, Alt JM, Bohle A, Stolte H: Kidney function and protein excretion in relation to pathomorphology of glomerular diseases. *Contrib Nephrol* 68: 128–135, 1988
3. Eddy AA, McCulloch L, Adams J, Liu E: Interstitial nephritis induced by protein-overload proteinuria. *Am J Pathol* 135: 719–733, 1989
4. The Gisen Group: Randomised placebo-controlled trial of effect of ramipril on decline in glomerular filtration rate and risk of

terminal renal failure in proteinuric, non-diabetic nephropathy. *Lancet* 349: 1857–1863, 1997
5. Wang Y, Chen J, Chen L, Tay Y-C, Rangan GK, Harris DCH: Induction of monocyte chemoattractant protein-1 in proximal tubule cells by urinary protein. *J Am Soc Nephrol* 8: 1537–1545, 1997
6. Zoja C, Morigi M, Figliuzzi M, Bruzzi I, Oldroyd S, Benigni A, Ronco PM, Remuzzi G: Proximal tubular cell synthesis and secretion of endothelin-1 on challenge with albumin and other proteins. *Am J Kidney Dis* 26: 934–941, 1995
7. Zoja C, Donadelli R, Colleoni S, Figliuzzi M, Bonazzola S, Morigi M, Remuzzi G: Protein overload stimulates RANTES production by proximal tubular cells depending on NF-κB activation. *Kidney Int* 1998, in press
8. Zager RA, Schimpf BA, Bredl CR, Gmur DJ: Inorganic iron effects on in vitro hypoxic proximal tubular cell injury. *J Clin Invest* 91: 702–708, 1993
9. Hirschberg R: Bioactivity of glomerular ultrafiltrate during heavy proteinuria may contribute to renal tubulo-interstitial lesions. *J Clin Invest* 98: 116–124, 1997
10. Olson JL, Hostetter TH, Rennke HG, Brenner BM, Venkatachalam MA: Altered glomerular permselectivity and progressive sclerosis following extreme ablation of renal mass. *Kidney Int* 22: 112–126, 1982
11. Edgington TS, Glassock RJ, Watson JI, Dixon FJ: Characterization and isolation of specific renal tubular epithelial antigens. *J Immunol* 99: 1199–1210, 1967
12. Read SM, Northcote DH: Minimization of variation in the response to different proteins of the Coomassie blue G dye-binding assay for protein. *Anal Biochem* 116: 53–64, 1981
13. Abbate M, Bachinsky D, Zheng G, Stamenkovic I, McLaughlin M, Niles JL, McCluskey RT, Brown D: Location of gp330/α 2-m receptor-associated protein (α 2-MRAP) and its binding sites in kidney: Distribution of endogenous α 2-MRAP is modified by tissue processing. *Eur J Cell Biol* 61: 139–149, 1993
14. McLean IW, Nakane PF: Periodate-lysine paraformaldehyde fixative: A new fixative for immunoelectron microscopy. *J Histochem Cytochem* 22: 1077–1083, 1974
15. Dijkstra CD, Dopp EA, Joling P, Kraal G: The heterogeneity of mononuclear phagocytes in lymphoid organs: Distinct macrophage subpopulations in the rat recognized by monoclonal antibodies ED1, ED2 and ED3. *Immunology* 54: 589–599, 1985
16. Kaissling B, Le Hir M: Characterization and distribution of interstitial cell types in the renal cortex of rats. *Kidney Int* 45: 709–720, 1994
17. Pichler R, Giachelli CM, Lombardi D, Pippin J, Gordon K, Alpers CE, Schwartz SM, Johnson RJ: Tubulointerstitial disease in glomerulonephritis: Potential role of osteopontin (uropontin). *Am J Pathol* 144: 915–926, 1994
18. Tokuyasu K: Immunocytochemistry on ultrathin frozen sections. *Histochem J* 12: 381–403, 1980
19. Kliem V, Johnson RJ, Alpers CE, Yoshimura A, Couser WG, Koch KM, Floege J: Mechanisms involved in the pathogenesis of tubulointerstitial fibrosis in 5/6-nephrectomized rats. *Kidney Int* 49: 666–678, 1996
20. Giachelli CM, Pichler R, Lombardi D, Denhardt DT, Alpers CE, Schwartz SM, Johnson RJ: Osteopontin expression in angiotensin II-induced tubulointerstitial nephritis. *Kidney Int* 45: 515–524, 1994
21. Eddy AA, Giachelli CM: Renal expression of genes that promote interstitial inflammation and fibrosis in rats with protein-overload proteinuria. *Kidney Int* 47: 1546–1557, 1995
22. Anderson S, Meyer TW, Rennke HG, Brenner BM: Control of glomerular hypertension limits glomerular injury in rats with reduced renal mass. *J Clin Invest* 76: 612–619, 1985
23. Anderson S, Rennke HG, Brenner BM: Therapeutic advantage of converting enzyme inhibitors in arresting progressive renal disease associated with systemic hypertension in the rat. *J Clin Invest* 77: 1993–2000, 1986
24. Cessac-Guillemet AL, Mounier F, Borot C, Bakala H, Perichon M, Schaeverbeke M, Schaeverbeke J: Characterization and distribution of albumin binding protein in normal rat kidney. *Am J Physiol* 271: F101–F107, 1996
25. Maack T, Park CH, Camargo MJF: Renal filtration, transport, and metabolism of proteins. In: *The Kidney: Physiology and Pathophysiology*, edited by Seldin DW, Giebisch G, New York, Raven, 1985, pp 1773–1803
26. Olbricht CJ, Cannon JK, Garg LC, Tisher CC: Activities of cathepsin B and L in isolated nephron segments from proteinuric and nonproteinuric rats. *Am J Physiol* 250: F1055–F1062, 1986
27. Nomura A, Morita Y, Maruyama S, Hotta N, Nadai M, Wang L, Hasegawa T, Matsuo S: Role of complement in acute tubulointerstitial injury of rats with aminonucleoside nephrosis. *Am J Pathol* 151: 539–547, 1997
28. Morita Y, Nomura A, Yuzawa Y, Nishikawa K, Hotta N, Shimizu F, Matsuo S: The role of complement in the pathogenesis of tubulointerstitial lesions in rat mesangial proliferative glomerulonephritis. *J Am Soc Nephrol* 8: 1363–1372, 1997
29. Zoja C, Corna D, Bruzzi I, Foglieni C, Bertani T, Remuzzi G, Benigni A: Passive Heymann nephritis: Evidence that angiotensin-converting enzyme inhibition reduces proteinuria and retards renal structural injury. *Exp Nephrol* 4: 213–221, 1996
30. Diamond JR, Kees-Folts D, Ricardo SD, Pruznak A, Eufemio M: Early and persistent up-regulated expression of renal cortical osteopontin in experimental hydronephrosis. *Am J Pathol* 146: 1455–1466, 1995
31. Pahl HL, Baeuerle PA: A novel signal transduction pathway from the endoplasmic reticulum to the nucleus is mediated by transcription factor NF-κB. *EMBO J* 14: 2580–2588, 1995